Asia-Pac. J. Atmos. Sci., 52(2), 223-236, 2016
DOI:10.1007/s13143-016-0021-0
pISSN 1976-7633 / eISSN 1976-7951

Changes of Precipitation Extremes over South Korea Projected by the 5 RCMs under RCP Scenarios

Joong-Bae Ahn[1], Sera Jo[1], Myoung-Seok Suh[2], Dong-Hyun Cha[3], Dong-Kyou Lee[4], Song-You Hong[5], Seung-Ki Min[6], Seong-Chan Park[7], Hyun-Suk Kang[8], and Kyo-Moon Shim[9]

[1]*Department of Atmospheric Sciences, Pusan National University, Busan, Korea*
[2]*Kongju National University, Kongju, Korea*
[3]*Ulsan National Institute of Science and Technology, Ulsan, Korea*
[4]*Seoul National University, Seoul, Korea*
[5]*Korea Institute of Atmospheric Prediction Systems, Seoul, Korea*
[6]*Pohang University of Science and Technology, Pohang, Korea*
[7]*Korea Meteorological Administration, Seoul, Korea*
[8]*National Institute of Meteorological Research, Jeju, Korea*
[9]*National Institute of Agricultural Science, Wanju, Korea*

(Manuscript received 31 October 2015; accepted 21 April 2016)

Abstract: The change of extreme precipitation is assessed with the HadGEM2-AO - 5 Regional Climate Models (RCMs) chain, which is a national downscaling project undertaken cooperatively by several South Korean institutes aimed at producing regional climate change projection with fine resolution (12.5 km) around the Korean Peninsula. The downscaling domain, resolution and lateral boundary conditions are held the same among the 5 RCMs to minimize the uncertainties from model configuration. Climatological changes reveal a statistically significant increase in the mid-21st century (2046-2070; Fut1) and the late-21st century (2076-2100; Fut2) precipitation properties related to extreme precipitation, such as precipitation intensity and average of upper 5 percentile daily precipitation, with respect to the reference period (1981-2005). Changes depending on the intensity categories also present a clear trend of decreasing light rain and increasing heavy rain. In accordance with these results, the change of 1-in-50 year maximum precipitation intensity over South Korea is estimated by the GEV method. The result suggests that the 50-year return value (RV50) will change from −32.69% to 72.7% and from −31.6% to 96.32% in Fut1 and from −31.97% to 86.25% and from −19.45% to 134.88% in Fut2 under representative concentration pathway (RCP) 4.5 and 8.5 scenarios, respectively, at the 90% confidence level. This study suggests that multi-RCMs can be used to reduce uncertainties and assess the future change of extreme precipitation more reliably. Moreover, future projection of the regional climate change contains uncertainties evoked from not only driving GCM but also RCM. Therefore, multi-GCM and multi-RCM studies are expected to provide more robust projection.

Key words: Regional climate change, CORDEX, extreme precipitation, RCP scenario, dynamical downscaling

1. Introduction

Global warming-induced precipitation change is one of the most important issues regarding human adaptation to climate change impact. The Fourth and Fifth Assessment Reports (AR4 and AR5) of the Intergovernmental Panel on Climate Change (IPCC) consistently estimate that heavy precipitation events are likely to increase in many areas worldwide, but with significant regional variations (Fowler et al., 2007; Gutowski et al., 2007; Sun et al., 2007; Im et al., 2008; O'Gorman and Schneider, 2009; Xu et al., 2009; Hanel and Buishand, 2011; Heinrich and Gobiet, 2011; Collins et al., 2013; Kirtman et al., 2013; Sillmann et al., 2013).

To investigate the climate change impact, global climate models (GCMs) are usually used to estimate future projections. However, GCMs have resolution problems to resolve the regional impact of climate change. To overcome this limitation, GCM projections that participated in the Coupled Model Inter-comparison Project Phase 5 (CMIP5; Taylor et al., 2012) are dynamically downscaled by Regional Climate Model (RCM) in many previous studies. Yu et al. (2015) used a representative concentration pathway (RCP; Moss et al., 2010) projection of the Model for Interdisciplinary Research on Climate version 5 as the boundary condition for the Weather Research and Forecasting (WRF) model to investigate the change of precipitation under RCP scenarios over mainland China. Emmanouil et al. (2013) also performed dynamical downscaling with WRF using historical projection of Institute Pierre Simon Laplace-CM5 GCM as the boundary condition to evaluate the added value of dynamical downscaling for Mediterranean surface winds and cyclonic activity. Moreover, despite its small territory, South Korea (hereafter, S. Korea) has complex orography with mixed features of mountainous areas and small islands (Im et al., 2006, 2007). Therefore, Regional Climate Model (RCM) study is indispensable for assessing the regional changes of extreme precipitation under global warming over S. Korea. In addition to RCM study, the ensemble approach is also important for investigating future

Corresponding Author: Sera Jo, Climate Prediction Laboratory, Department of Atmospheric Sciences, Pusan National University, Gumjung-gu, Jangjeon-dong, Busan 46241, Korea.
E-mail: seta43@pusan.ac.kr

changes. Generally, climate models have different systematic biases arising from numerical schemes and physical parameterizations. Accordingly, different climate models can respond to the same forcing differently and present diverse evolution of future projection. Therefore, an ensemble approach can give a range of possible futures and reveal the uncertainties of the projections (Collins et al., 2013).

The emphasis on regional downscaling and the ensemble approach has led to the instigation of an international project named the Coordinated Regional Climate Downscaling Experiment (CORDEX), which is a global project of the World Climate Research Program among various worldwide institutes. They define common domains and configurations to control the uncertainties from domains or resolutions and secure unity among experiments over the same domain. However, the 50-km horizontal resolution of the CORDEX East Asia domain, which includes S. Korea, remains insufficient for resolving extreme events over the complex and narrow Korean Peninsula.

Consequently, a multi-RCM ensemble project has been designed by National Institute of Meteorological Research (NIMR) under the Korea Meteorological Administration (KMA), which participated in the CMIP5 with HadGEM2-AO simulations forced by RCP scenarios (Baek et al., 2013). With this RCP projection of HadGEM2-AO, 5 RCMs performed dynamical downscaling in cooperation with several Korean research groups. Seo et al. (2015) assessed the changes in extreme rainfall in S. Korea with the HadGEM2-AO - HadGEM3-RA model chain and found that the return period of the 50-year return value will decrease to 1-in-16 year. Meanwhile, Im et al. (2015) have postulated an increased return value in 1-in-20 year and 1-in-50 year with WRFv3.4. However, these studies were limited by their use of only one GCM-RCM chain and the multi-RCM results have not yet been assessed for future projection over S. Korea in terms of extreme precipitation with fine resolution less than 20 km. In this study, we analyzed 5 different dynamically downscaled results from 5 RCMs that have all different dynamical cores and combinations of physical schemes. Fowler et al. (2007) insisted that although the magnitude of change comes from driving GCM, the spatial pattern can be moderated by RCMs when projecting future climate using the GCM-RCMs model chain. Jankov et al. (2005) showed that a different combination of physical parameterizations can efficiently ensure a sufficient ensemble spread. Therefore, comparing different RCMs with different combinations of physical schemes is expected to give sufficient ensemble spread and enough information about the uncertainty of the projected extreme precipitation although the lateral boundary condition is from one driving GCM.

In this study, we investigate the performance of RCMs on precipitation and examine the future changes of general precipitation properties under RCP scenarios. Finally, we assess the changes of extreme precipitation projected by the 5 RCMs model chained by 1 GCM and show the range of change in future projection over S. Korea.

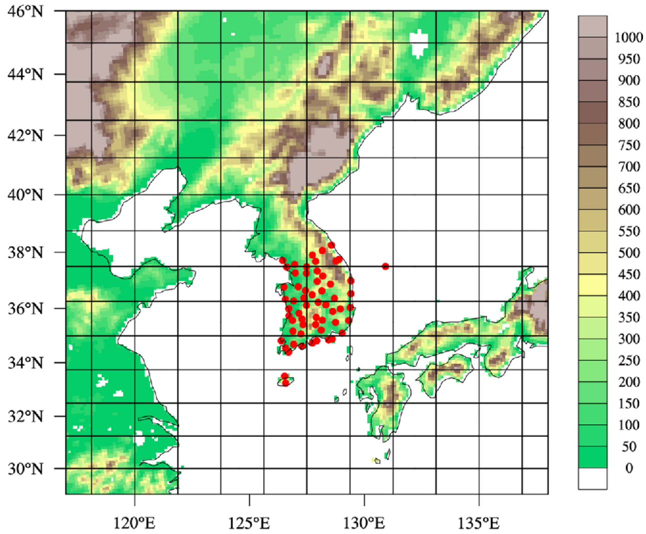

Fig. 1. RCMs simulation domain and ASOS locations (red dots). Mesh lines are grids of HadGEM2-AO.

2. Model descriptions and data

The fine resolution RCP scenarios for around the Korean Peninsula are produced by dynamical downscaling with 5 different RCMs. To exclude external factors that can affect the result of dynamical downscaling, all models are set to the same domain (Fig. 1) and horizontal resolution 12.5 km. The configurations of the 5 RCMs are different from each other with different combinations of dynamic frame work, planetary boundary layer scheme, convective scheme, and spectral nudging. Table 1 summarizes the model configuration for each RCM. The lateral boundary condition for the RCMs is HadGEM2-AO Historical and RCP4.5/8.5 projections. HadGEM2-AO is a climate model composed of an atmospheric general circulation model with N96 ($1.875^o \times 1.25^o$) horizontal resolution and 38 vertical levels and an oceanic general circulation model with zonally 1^o, meridionally 1^o between the poles and 30^o latitude from which it increases smoothly to $1/3^o$ at the equator for horizontal resolution and 40 vertical levels (Baek et al., 2013). The model also includes other components of the earth system such as terrestrial and oceanic carbon cycle and tropospheric chemistry (Martin and Levine, 2012). The RCP scenarios run with two kinds of simulation: the Historical scenario which represents the current climate and the RCPs which project the future climate under emission forcing. For the Historical experiment, from 1979 to 2005, 27 years are simulated but only 25 years from 1981 to 2005 (hereafter, REF) are used for analysis since the first two years are regarded as the spin-up period. In the RCP4.5 and RCP8.5 experiments, the simulation period runs 82 years from 2019 to 2100. The 25 years of 2046 to 2070 are assigned to the mid-21st century (hereafter, Fut1) and those of 2076 to 2100 to the late 21st century (hereafter, Fut2). To assess the changes of extreme precipitation, daily observational data from the 60

Table 1. The configuration of the 5 RCMs. Names in parentheses under the RCM name denote the institutes that produced the data. NIMR, UNIST, KNU, POSTECH and PNU represent National Institute of Meteorological Research, Ulsan National Institute of Science and Technology, Kongju National University, Pohang University of Science and Technology and Pusan National University, respectively.

Models (Institute)	HadGEM3-RA (NIMR)	SNURCM (UNIST)	RegCM4 (KNU)	GRIMs (POSTECH)	WRFv3.4 (PNU)
Horizontal Resolution (lat × lon)	12.5 km (180 × 200)	12.5 km (180 × 201)	12.5 km (180 × 200)	12.5 km (182 × 201)	12.5 km (180 × 200)
Vertical layer (model top)	Hybrid-38 (40 km)	24 sigma (70 hPa)	23 sigma (50 hPa)	28 sigma (3 hPa)	28 Eta (50 hPa)
Dynamic framework	Non-hydrostatic	Non-hydrostatic	Hydrostatic	Hydrostatic	Non-hydrostatic
PBL scheme	Nonlocal scheme	YSU	Hotslag	YSU + stable BL	YSU
Convective scheme	Revised mass flux scheme	Kain-FritchII	MIT-Emanuel	SAS + CMT	Kain-Fritsch
Land surface model	MOSES-II	CLM3.0	CLM3.5	OML climatology	NOAH
Short/Long wave radiation scheme	Generalized 2-stream	CCM2	CCM3	GSFC	CAM
Spectral nudging	No	Yes	Yes	Yes	No

Automated Surface Observing System (ASOS) of KMA during the REF period are used. We compare the observation and model results using the nearest model grid point of each station location without any objective interpolations since the horizontal resolution (12.5 km) of our experiment was sufficient for comparison with ASOS (Average distance between an ASOS site to the other nearest sites : 32.6 km).

3. Extreme value analysis

Generalized Extreme Value (GEV) analysis is performed to assess the change of extreme precipitation over S. Korea. The GEV method fits the extreme values on a GEV distribution by combining three types of cumulative distribution function - Gumbel, Frechet and Weibull - and estimates the extreme values for the given return period (or estimates the return period for given certain value) (Fisher and Tippett, 1928). Many previous studies used this method to investigate various extreme phenomena in meteorology (Fowler et al., 2007; Zweirs et al, 2011; Im et al., 2015; Seo et al., 2015).

Two general ways are used to fit extreme values into a GEV distribution: Maximum likelihood and L-moments method (Hosking and Wallis, 1997; Wilks, 2011). We use the latter because of its greater suitability for smaller samples than the former. The annual maximum series of daily precipitation is extracted throughout all five RCMs during REF, Fut1 and Fut2 periods and fitted into the GEV distribution using L-moments over 60-station locations point by point.

4. Results

a. Model Evaluation on precipitation

Before investigating extreme precipitation, we assess the performance of each RCM on precipitation by comparing bias and RMSE during the REF period. Table 2 shows the annual and seasonal mean daily precipitation bias and Root Mean Square Error (RMSE) of the 5 RCMs with respect to ASOS. ASOS shows annual mean daily precipitation of about 3.66 mm d^{-1}, with a maximum seasonal mean of 7.71 mm d^{-1} in the summer. Since, the Korean Peninsula is affected by the East Asian monsoon, approximately 60-65% of annual precipitation falls in the summer months of June-August. Accordingly, annual maximum precipitation is usually recorded during warm season from late June to early September related to convective storms or mesoscale convective systems associated with Changma front or typhoons (Lee et al., 1998). However, HadGEM2-AO has the largest dry bias in the wet season of S. Korea. This implies that the GCM will likely underestimate

Table 2. Annual and seasonal mean bias and RMSE of precipitation (unit: mm d^{-1}) in reference period.

		Annual	Spring	Summer	Fall	Winter
ASOS	Mean	3.66	2.43	7.71	2.88	1.19
HadGEM2-AO	Bias	–0.75	0.63	–2.17	–0.14	–0.19
	RMSE	0.75	0.51	2.65	0.85	0.24
HadGEM3-RA	Bias	–0.32	1.5	–1.74	0.19	–0.12
	RMSE	0.38	0.99	1.91	0.52	0.22
SNURCM	Bias	–0.29	0.58	–1.81	0.29	0.25
	RMSE	0.48	0.59	1.82	0.49	0.57
RegCM4	Bias	–0.75	0.4	–2.64	–0.38	0.05
	RMSE	0.77	0.39	2.69	0.76	0.32
GRIMs	Bias	–0.21	0.65	–2.21	0.85	0.38
	RMSE	0.57	0.53	1.85	0.5	0.65
WRFv3.4	Bias	0.37	1.27	–1.19	1.07	0.93
	RMSE	0.57	1.22	1.44	0.56	1.27

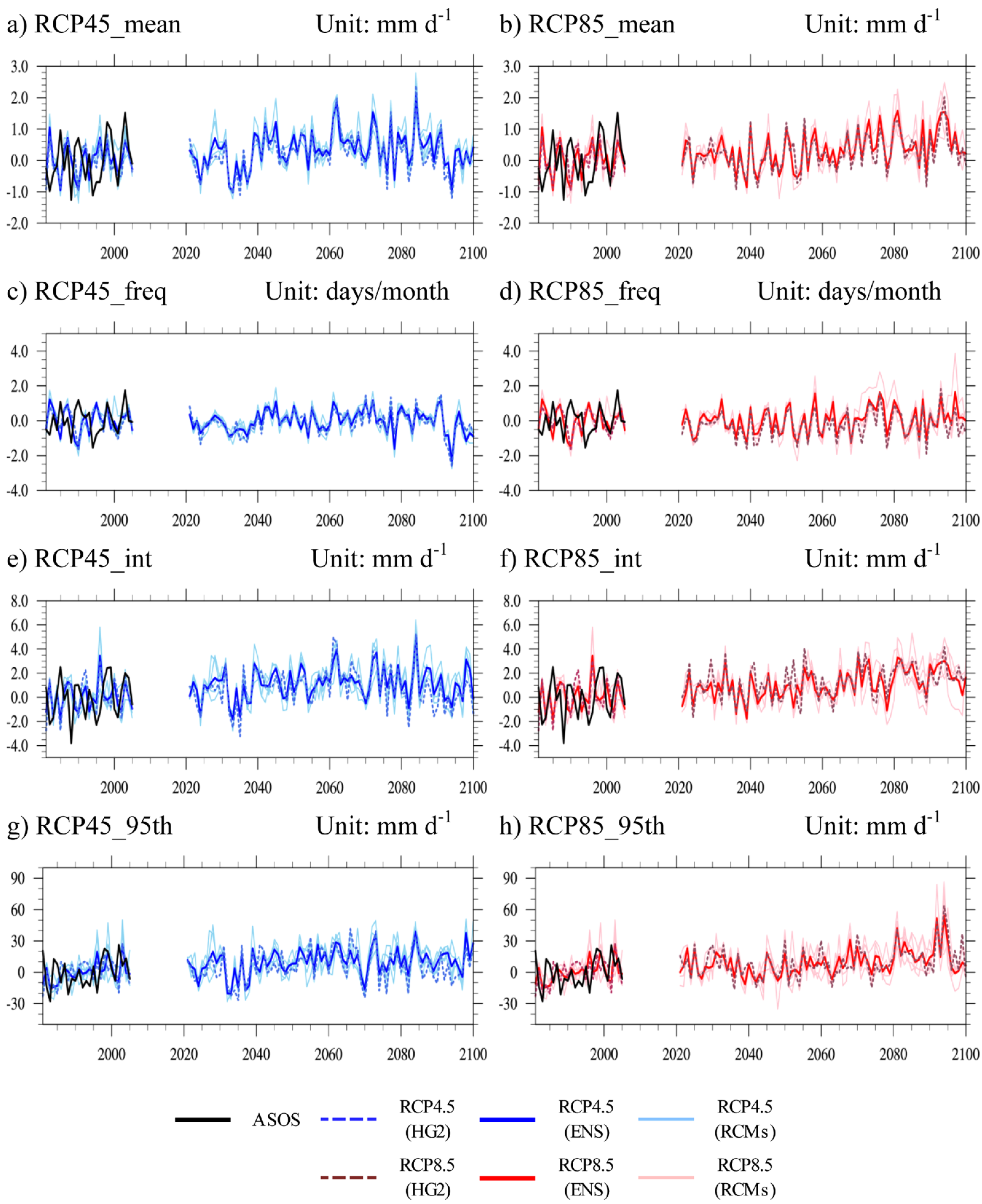

Fig. 2. Time-series of annual mean precipitation anomaly (mm d^{-1}) for a) RCP4.5 and b) RCP8.5. Second row shows the annual mean frequency of precipitation event for c) RCP4.5 and d) RCP8.5. Third row shows the annual mean of precipitation intensity for each scenario. Bottom row shows the annual mean of upper 5 percentile precipitation. Thin and thick solid lines are the time-series of the individual RCMs and ensemble mean, respectively. The dashed lines are for the HadGEM2-AO results.

the extreme precipitation compared to observed precipitation. Similarly, RMSE is bigger in summer (2.65) than in the other seasons (0.24-0.85). Despite these errors, Hong and Ahn (2015) showed that this bias and RMSE of HadGEM2-AO in summer precipitation are relatively less than those of CMIP5 multi-model ensemble. After dynamical downscaling, most RCMs show a similar result of decreased annual bias and RMSE compared with HadGEM2-AO except for RegCM4

Table 3. The average, inter-annual standard deviation and changes of average value from reference period. All values are calculated from ensemble mean of RCMs with simple composite method during 25 years of each period. Asterisks show the t-test results for difference. *significance level: 5%, **significance level: 1%.

		average	stddev	difference
Average	historical	3.42	0.52	-
	RCP45_Fut1	3.89	0.48	0.47**
	RCP45_Fut2	3.76	0.65	0.34
	RCP85_Fut1	3.62	0.52	0.20
	RCP85_Fut2	4.07	0.60	0.65**
Frequency	historical	8.53	0.72	-
	RCP45_Fut1	8.64	0.53	0.10
	RCP45_Fut2	8.00	0.86	−0.53*
	RCP85_Fut1	8.41	0.79	−0.13
	RCP85_Fut2	8.74	0.84	0.21
Intensity	historical	11.06	1.21	-
	RCP45_Fut1	12.33	1.05	1.28**
	RCP45_Fut2	12.23	1.40	1.18**
	RCP85_Fut1	11.93	1.02	0.87*
	RCP85_Fut2	12.81	1.08	1.75**
95th average	historical	75.88	10.23	-
	RCP45_Fut1	87.55	10.49	11.67**
	RCP45_Fut2	91.29	10.94	15.41**
	RCP85_Fut1	82.78	9.99	6.90*
	RCP85_Fut2	92.28	14.95	16.40**

(RMSE increased about 0.02). That is, RCMs simulate more precipitation than GCM and this relieves the dry bias of the global model. Seasonally, the performance of summer precipitation is improved but that of winter time shows an increment of wet bias. This can be interpreted as the impact of more realistic and detailed orography in RCMs (Im et al., 2006), which is related with the heavy winter snowfall in the mountainous areas. However, all models still show a negative bias in summer, which was ascribed to HadGEM2-AO. Meanwhile, although 5 RCMs use the same lateral boundary condition, their different characteristics make their own climatology of precipitation model by model, this may lead to diverse estimation of extreme precipitation.

Consequently, HadGEM2-AO and RCMs model chains describe the seasonal cycle of the precipitation over S. Korea similar with ASOS and dry bias of global model reduced after dynamical downscaling in summer which is a season of heaviest rain fall in S. Korea. Further, it is suggested that 5 RCMs have different characteristics in describing the seasonal variation of precipitation as shown in observation (Table 2). Referring to the basic performance of the HadGEM2-AO and the 5 RCMs in terms of model bias and RMSE, we further investigated the future change of daily precipitation and extreme events and assessed the uncertainties of the projections.

b. Future change of precipitation characteristics

To investigate the long-term change of precipitation characteristics, we analyze the time series of anomaly for annual mean, frequency, intensity and upper 5 percentile of precipitation over S. Korea (Fig. 2) averaged over the 60 stations. In this study, in order to prevent the characteristics of extreme values from being smoothed out and dominated by a certain RCM which has large variability, the ensemble-averaged results are not used for the analysis. However, the ensemble-averaged results are used only in Table 3 and Fig. 2 because of readability. Precipitation events are defined as a daily precipitation of more than 0.1 mm d^{-1}. We derive the anomaly by subtracting the climatology of the ensemble average during the REF period from the ensemble average of the 5 RCMs during RCP future projections to extract the systematic bias. Generally, systematic bias is defined as the mean state difference between model and observation. The systematic bias is easily removed by extracting model climatology (Kug et al., 2008; Ahn et al., 2012). The ensemble method used here is the simple composite method (Peng et al., 2002; Jeong et al., 2012; Kryjov, 2012; Lee et al., 2013a, 2013b). Statistics such as the average and the standard deviation for each period (25-yearlong) are summarized in Table 3. The annual mean precipitation and frequency are presented in Figs. 2a-d for RCP4.5 and RCP8.5 scenarios, respectively. Over the whole simulation period, there is no significant trend such as temperature response for greenhouse gas (GHG) forcing, neither for the mean precipitation nor for the precipitation frequency, in either RCP 4.5 or RCP 8.5, as shown in the IPCC AR5 working group I (Collins et al., 2013; Kirtman et al., 2013) and previous studies with HadGEM2-AO and RCM model chain (Hong et al., 2013; Ahn et al., 2014; Lee et al., 2014; Im et al., 2015). This indicates that precipitation, in contrast to temperature, does not respond to radiative forcing linearly, as pointed out in Shindell et al. (2012). However, in the climatological viewpoint, the average of annual mean precipitations during RCP4.5 Fut1 and RCP8.5 Fut2 show a significant increase at the 99% confidence level. For precipitation frequency, only RCP4.5 Fut2 shows a significant decrease of climatology at 95% confidence level (Table 3). This increase of mean precipitation during RCP4.5 Fut1 and RCP8.5 Fut2 and decrease of frequency in RCP4.5 Fut2 may result in increase of precipitation intensity. Figures 2e-h are the annual mean precipitation intensity and heavy rain intensity (average of upper 5 percentile daily precipitation per year, hereafter, 95th precipitation). Both RCP4.5 and 8.5 scenarios show that annual mean precipitation intensity and heavy rain intensity will increase over S. Korea significantly which is consistent with previous studies (Im et al., 2011, 2012, 2015; Lee et al., 2014; Oh et al., 2014; Hong and Ahn, 2015). The changes in climatology are also significant at 95% confidence level or higher in all periods. Moreover, the increased inter-annual

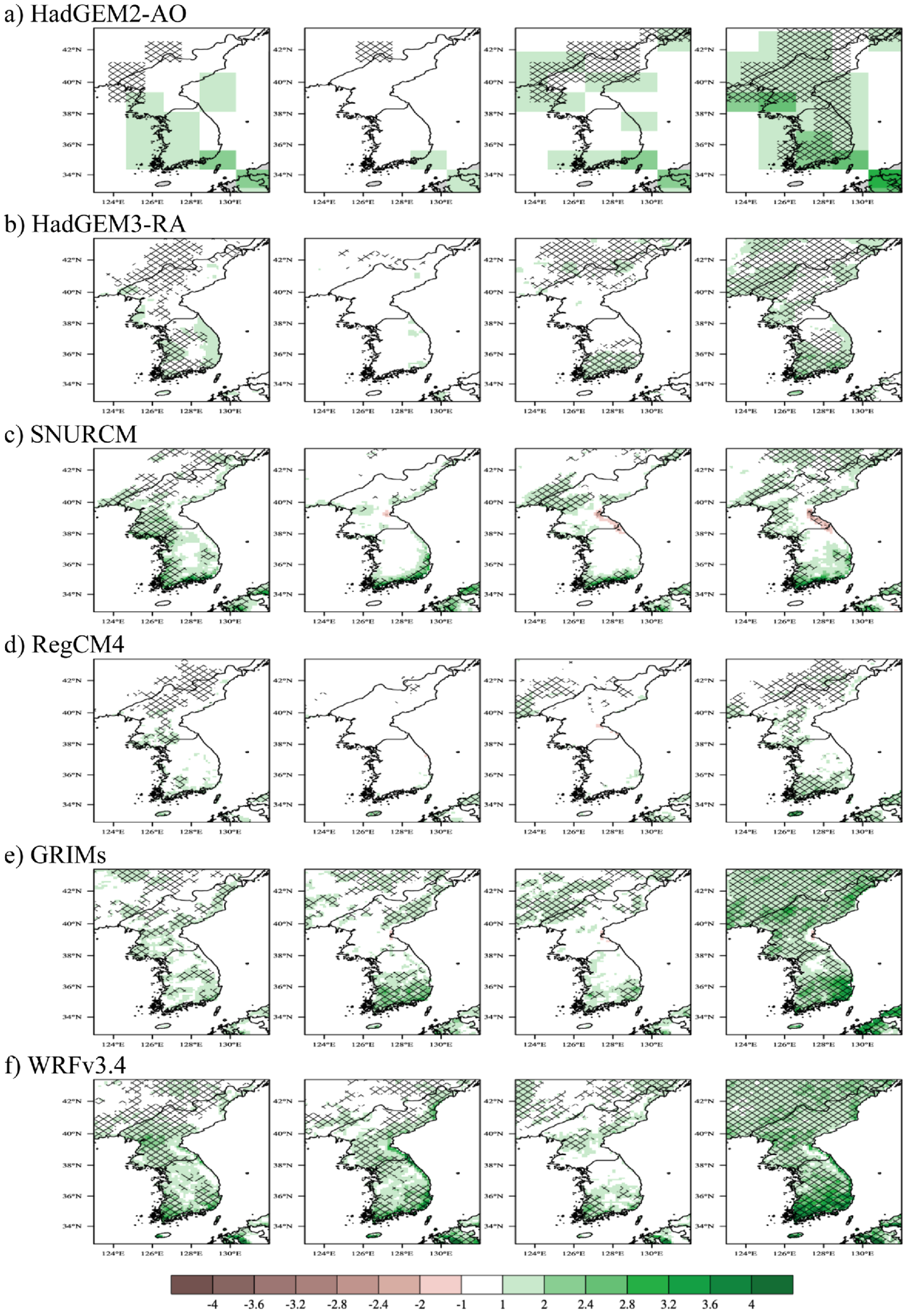

Fig. 3. Annual mean precipitation intensity (unit: mm d^{-1}) difference of RCP scenarios with respect to the reference period projected by a) HadGEM2-AO, b) HadGEM3-RA, c) SNURCM, d) RegCM4, e) GRIMs and f) WRFv3.4. The left most two panels are for RCP4.5 Fut1 and Fut2 and the next two are for RCP8.5 Fut1 and Fut2 in the order left to right. The hashed area denotes the changes that are statistically significant at the 95% confidence level.

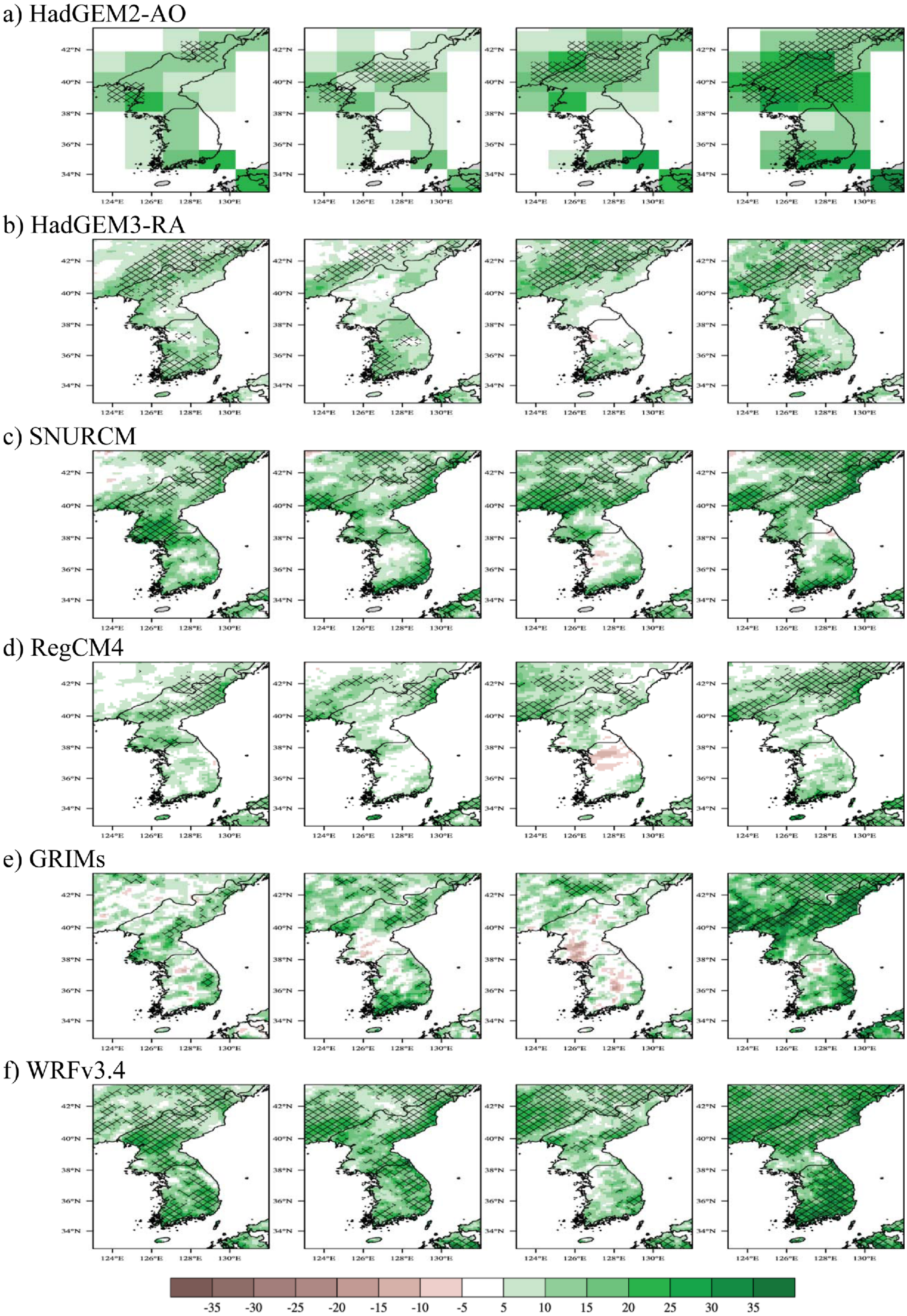

Fig. 4. Same as Fig. 3 but 95th precipitation (unit: days).

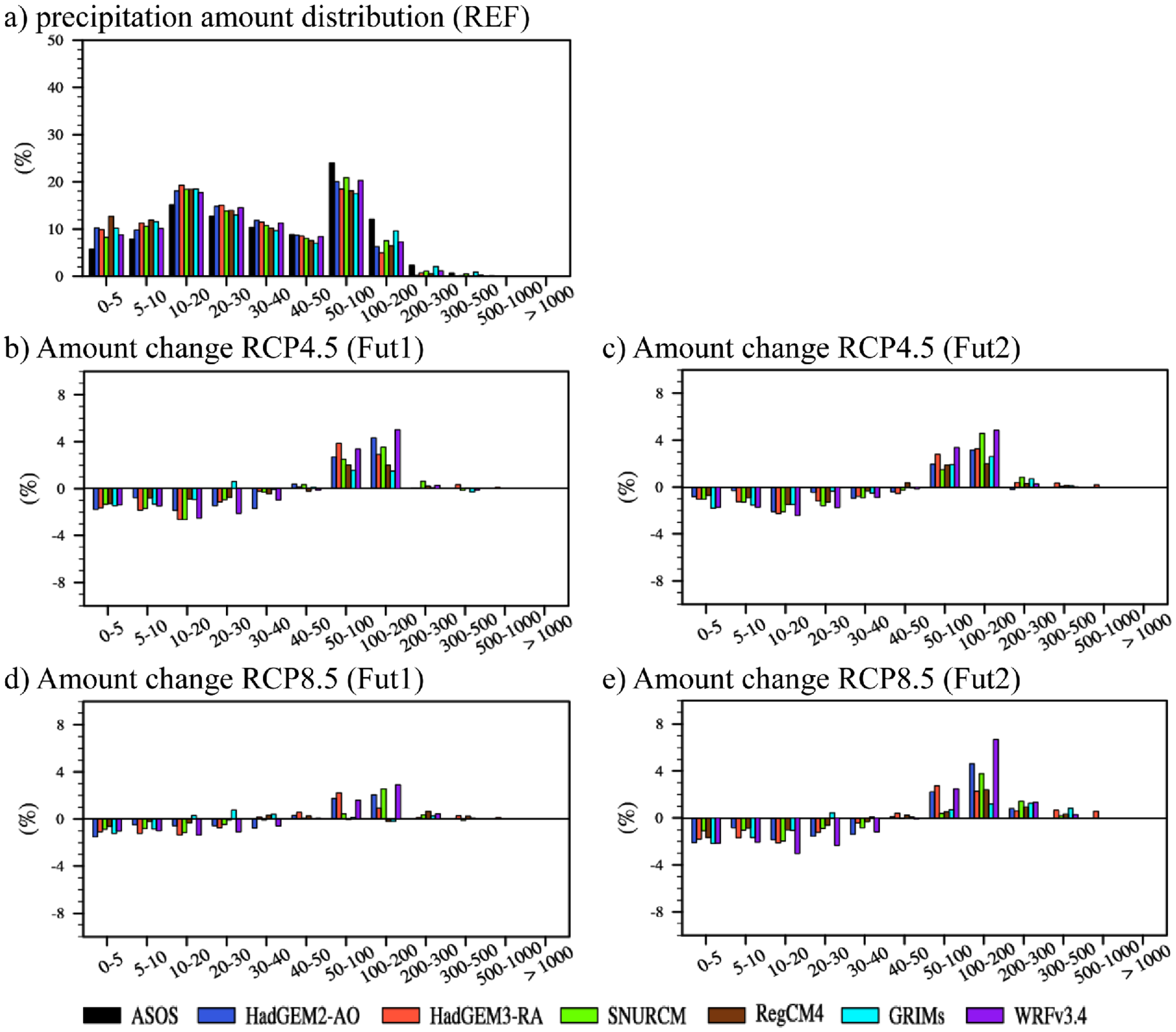

Fig. 5. Probabilistic distribution of precipitation quantity with respect to precipitation intensity derived from a) ASOS and Historical projection. For future projections, amount changes (%) during b) RCP4.5 Fut1, c) RCP4.5 Fut2, d) RCP8.5 Fut1 and e) RCP8.5 Fut2 over 60 stations.

variation of heavy rain intensity is evident in RCP8.5 Fut2. Therefore, the probability of extreme events is projected to increase in both Fut1 and Fut2 based on RCP4.5 and RCP8.5 scenarios.

Meanwhile, Fig. 2 shows a common characteristic in that the spread between the RCMs increases as the simulation progresses in the historical period. In addition, RCP 8.5 shows a broadened ensemble spread, especially after the 2070's. Therefore, a larger uncertainty of extreme precipitation is expected under RCP 8.5 scenario than under RCP4.5, which is reminiscent of the need for an ensemble approach to investigate the projection of extreme precipitation.

Although we found that enhanced heavy rain is expected in future under RCP scenarios through time series analysis, it is revealed that uncertainties exist not only in time evolution but also spatial pattern. Therefore, we analyze the spatial distribution of precipitation intensity and the 95th precipitation changes with respect to the REF period for each model. The precipitation intensity of HadGEM2-AO is projected to increase over the Korean Peninsula in Fut2 of RCP8.5 and Fut1 of RCP4.5 scenario (Fig. 3). The RCMs show a different spatial pattern of intensity change, although the most significant increase of intensity over S. Korea is shown in RCP8.5 Fut2 in accordance with HadGEM2-AO. Also, the model spread is distinct in the period. RegCM4 and SNURCM project a similar level of precipitation intensity with the REF period, whereas HadGEM3-RA, GRIMs and WRFv3.4 show clear increment. In RCP4.5 Fut2 and RCP8.5 Fut1, the results differ from model to model, but the south coastal regions tend to be included in regions with statistically significant change. According to Fig. 4 showing the change of 95th precipitation, almost the whole domain shows enhanced intensity of heavy rain events. However, some RCMs present decreased heavy rain around the middle of the Korean peninsula, especially in

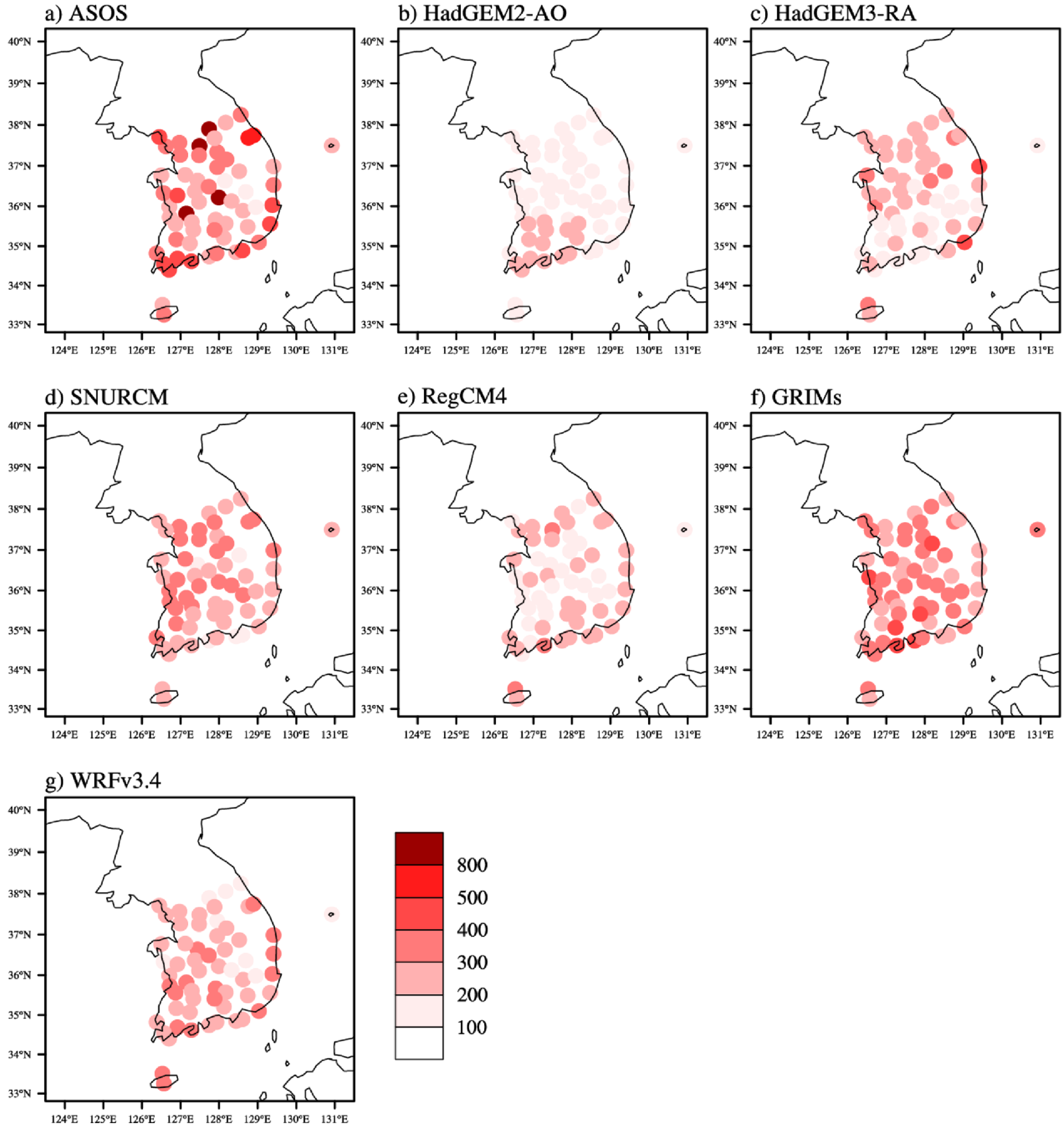

Fig. 6. Spatial distribution of RV50 (unit: mm d^{-1}) in the REF period for observation and each model.

RCP8.5 Fut1. This characteristic appears to be inherited from HadGEM2-AO.

The time series and spatial distribution of precipitation changes suggest that precipitation, especially heavy rain intensity, tends to be increased under RCP scenarios. Moreover, enhanced heavy rain is directly associated with extreme value estimation. To investigate these changes more quantitatively, the precipitation is classified according to various intensity categories. Figure 5a shows the probabilistic distribution of precipitation amount depending on the precipitation intensity and percentage during the REF period. Figures 5b-e show changes in precipitation amount for each scenario and future period. As shown in Fig. 5a, in general, the GCM and RCMs clearly follow the distribution of ASOS. However, light rain less than 50 mm d^{-1} is overestimated whereas heavy rain is slightly underestimated, as is typical with all climate models (Frei et al., 2003; Mehran et al., 2014). Comparing GCM and RCMs, the RCM results are closer to the observation than GCM for heavy precipitation over 50 mm d^{-1}. These results are consistent with previous studies (Harding et al., 2013; Lee and Hong, 2014; Dosio et al., 2015), and represent the added value of dynamical downscaling in projecting extreme precipitation events. Moreover, since the right tail of PDF is the decisive factor to estimate the extreme values in the GEV analysis, realistic extreme values can be more easily estimated with RCMs than with GCM. The future change perspective exhibits a clear trend of decreasing light precipitation and increasing heavy rainfall regardless of the scenarios and periods. HadGEM2-AO and the 5 RCMs show almost the same changes in probabilistic distribution of precipitation intensity: decreased light rain and increased heavy rain. This indicates that more intense and frequent floods are projected over S. Korea in the future compared to the Historical period. In comparing RCP4.5 and RCP8.5, the former shows more notable increase of heavy precipitation in Fut1 than in Fut2, whereas RCP8.5 shows the opposite trend. This trend seems to be consistent with the radiative forcing trend of each RCP scenario: RCP4.5 scenario shows radiative forcing growth from 2000 to the 2050s up to 4.5 W m^{-2} and then stabilizes until the end of the 21st century, whereas RCP8.5 maintains a sharp increase from 2000 to the end of the 21st century up to 8.5 W m^{-2} (see Fig. 4 of Meinshausen et al., 2011). The amplitude of WRFv3.4 is the largest among all RCMs, but HadGEM3-RA shows an increased sign in the strongest intensity criteria in all cases. This could impact on the extreme value estimation result in section 4.c.

The general characteristics of precipitation projected by this model chain show that intense and heavy precipitation over S. Korea is expected to be increased under RCP scenarios. However, there exists an ensemble spread not only in temporal evolution but also in the spatial pattern of precipitation features such as intensity and 95th precipitation. Thus, extreme value analysis is applied to each model separately to avoid the smoothing effect and maintain the variation and characteristics of individual model.

c. Future change of extreme precipitation event

To assess how the RCMs project extreme precipitation, apply the GEV method on projected precipitation. The GEV method uses a series of annual maximums during analysis period and estimates the return value and return period by fitting the series onto the GEV distribution. The return value of 1-in-N years represents for the precipitation intensity that exceeds a probability of 1/N in the GEV distribution of annual maxima. In this section, we firstly examine the GEV result spatially with respect to 1-in-50 years return value (hereafter, RV50) in the historical period (Fig. 6). Because of the model deficiency that underestimates heavy rain, RV50s of models are generally smaller than those of ASOS. The maximum RV50 of ASOS is 1073.33 mm d^{-1} and it shows relatively high intensity precipitation over the northwestern part and coastline of S. Korea. Meanwhile, RV50 projected by HadGEM2-AO was relatively smaller than that of ASOS, which was expected because of the characteristic underestimation of heavy rain, as shown in Fig. 5a. Moreover, the spatial distribution of RV50 from GCM is rougher than that of ASOS because of the coarse

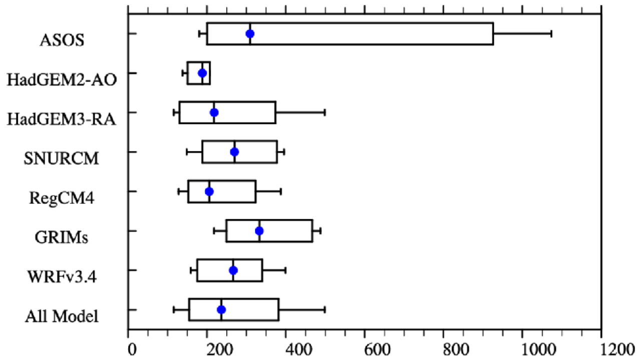

Fig. 7. Box plot of RV50 (mm d^{-1}) for 60 stations over S. Korea during the REF period. The boxes indicate 90% confidence intervals. The blue dots show the median, while upper and lower whiskers denote the minimum and maximum values among the 60 stations, respectively. The "All Model" box plot is derived from 300 values pooling 60 stations of each of the five RCMs.

resolution of HadGEM2-AO, which covers S. Korea with only a few grid points (Fig. 1). Nevertheless, this discrepancy is reduced after dynamical downscaling in terms of intensity and spatial distribution. RV50s downscaled by RCMs have stronger intensity and more detailed spatial distribution than those by GCM, but still show smaller intensity than ASOS. In addition, the spatial distributions of RV50s show no agreement between models or with ASOS. This highlights the considerable uncertainties inherent in assessing the risk of climate change with few ensemble members. Therefore, this study investigates the range of RV50 over S. Korea rather than the deterministic value at each station location. Figure 7 shows the box plot of RV50 for 60 stations over S. Korea during the REF period. The blue dot of each box represents the median value among 60 values, while the upper and lower whiskers indicate the maximum and minimum values, respectively. The edges of each box represent the upper and lower 5th percentile, so that the range of the box can be interpreted as the 90% confidence interval for RV50 throughout S. Korea. ASOS has a median of 220 mm d^{-1} and shows a wide range from median to maximum value and the lower edge of the box is almost 200 mm d^{-1}. This denotes that the annual maximum intensity of daily precipitation that returns in 50 years will evoke a flood over 95% of the 60 stations in S. Korea. However, HadGEM2-AO does not show these characteristics and has a small range of RV50. RCMs show a wider range of RV50 than GCM does, although still smaller than that of ASOS. The median values of each model differ because of bias. To summarize the ensemble members, simply averaging the 5 RCMs can smooth out the characteristic of extreme precipitation because all models show different spatial distributions and ranges of RV50 in Fig. 6. Therefore, we pool the 300 values from 60 station RV50 values of the 5 different RCMs and draw a box plot termed "All Model" in Fig. 7. The resulting median value of 210 mm d^{-1} is similar to that of ASOS (220 mm d^{-1}) and the range at 90% confidence level is about 150-400 mm d^{-1}, which is still narrower than that of ASOS. Therefore, we should

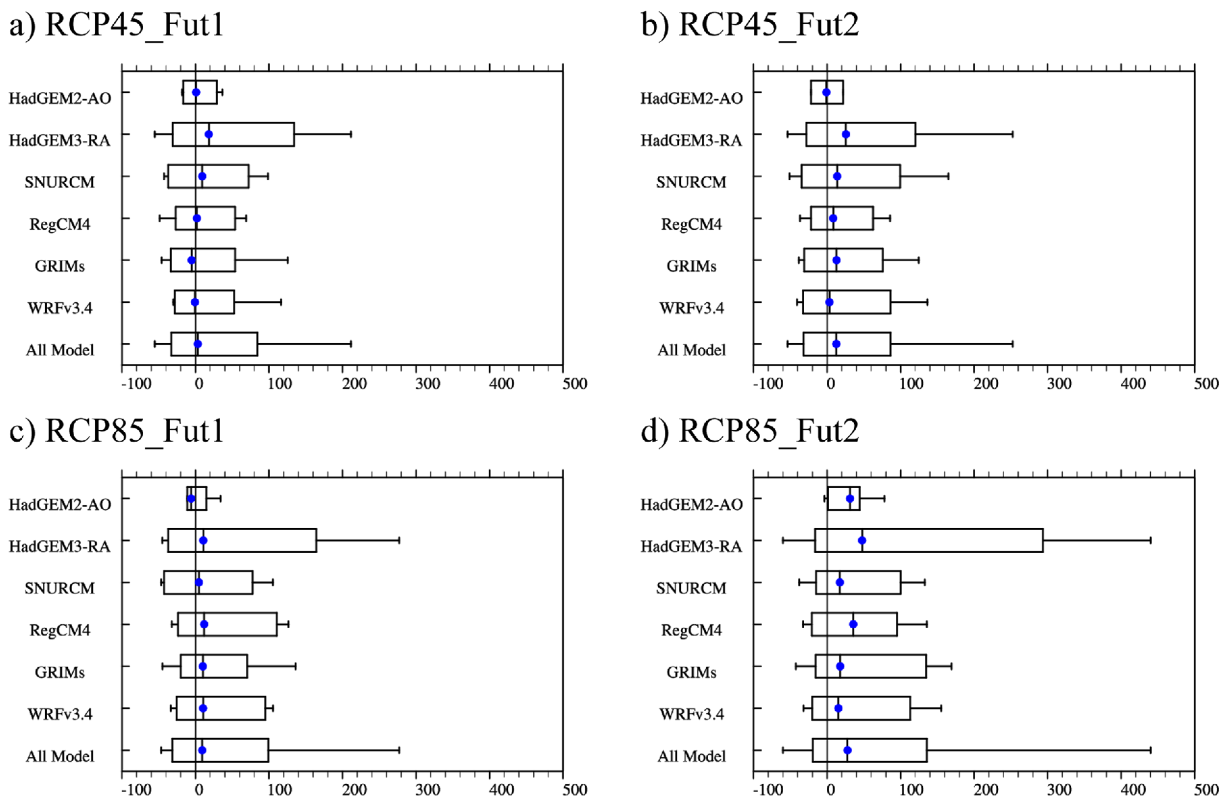

Fig. 8. Box plot of return value change (%) with respect to the REF period. The boxes indicate 90% confidence intervals for the 5 RCMs and Ensemble.

consider this limitation of GCM and the RCMs in the future projections as well as in the REF period.

During the reference period, relatively high vulnerability is presented around the coastal regions and western province. However, these characteristics are not always in accordance among 5 RCMs. Moreover, the quantitative discrepancies exist among each RCM, which are attributed to the model characteristics and bias. However, bias correction in future projection studies remains controversial (Chen et al., 2011; Ehret et al., 2012; Teutschbein and Seibert, 2012a, 2012b). Especially, Chen et al. (2011) stated that the choice of bias correction method can be an additional source of uncertainty. Therefore, we derive the change ratio (%) of return value with respect to REF rather than applying bias correction to the comparison of each model together in the same level (Fig. 8). The equation for change ratio (%) is as follow:

$$\text{change}~(\%) = \frac{(RV50_{Fut} - RV50_{REF})}{(RV50_{REF})} \times 100 \qquad (1)$$

The $RV50_{REF}$ indicates the RV50 value for the reference period and $RV50_{Fut}$ is that of the Fut1 or Fut2 period. Figure 8 shows the box plots for changes of extreme precipitation over S. Korea during the Fut1 and Fut2 periods for both RCP4.5 and RCP8.5 scenarios. The edges of each box represent the 90% confidence interval for RV50 change over S. Korea. A median of greater than 0 indicates that more than 50% of stations present an increased RV50 under RCP scenarios. HadGEM2-AO shows that the median value is almost the same with the REF period under RCP4.5 scenario in both the Fut1 and Fut2 periods. Under RCP8.5 scenario, it projected a decreased median during Fut1 and an increased median in Fut2 (31.22%) and the upper whisker increased to 77.96%.

Summarizing the result of RV50 change according to each model, a large spread is clearly evident in extreme precipitation projection, although we make RCM ensemble from one 1 driving GCM. Therefore, from the 5 RCM's projection results, we present the changes of extreme precipitation over S. Korea in range (Fig. 8). The edges of each box represents upper and lower 5th percentile. That means, the range of the box can be interpreted as the 90% confidence interval for RV50 change throughout S. Korea. A median of greater than 0 indicates that more than 50% of stations are expected to present an increased RV50 under RCP scenarios. In this sense, GRIMs (−5.17) and WRFv3.4 (−0.6) of RCP4.5 Fut1 project RV50 decreased by more than 30 stations. The medians of RCP8.5 Fut2 are the largest among the other periods. HadGEM3-RA shows the widest 90% confidence interval in the 5 RCMs and the largest median appears in RegCM4 during RCP8.5 Fut2. Furthermore, the median and upper whisker tend to be increased and the lower whisker decreased more under heavy emission forcing, which indicate that regional variation tends to increase under warmer climate. Also, 5 RCMs coincide in that more intense extreme precipitation is expected over more than half of S. Korea under RCP scenarios except for RCP4.5 Fut1 period. To summarize the different results of the 5 RCMs, we pool the 5 RCMs' RV50 changes into one and calculate the median and 90% confidence interval (represented as "All Model" in the Y-axis of Fig. 8). For the median, Fut2 period shows a slightly increased value compared to Fut1 under both RCP4.5 and RCP8.5 and the most relevant increase is projected during Fut2 period of RCP8.5 scenario. In Fut1, the 1-in-50 year precipitation intensity is projected to be changed from −32.69% to 72.7% with respect to present with RCP 4.5 scenario and from −31.6% to 96.32% for RCP8.5 scenario at the 90% confidence level from the HadGEM2-AO - 5RCMs model chain over S. Korea. The median is expected to be increased about 3.25% in RCP4.5 scenario and 9.25% in RCP8.5 scenario. At the Fut2, RV50 is expected to be changed from −31.97% to 86.25% compared to the reference period under RCP4.5 scenario and from −19.45% to 134.88% with RCP8.5 scenario at the 90% confidence level under the HadGEM2-AO - 5RCMs model chain. The median is also expected to be increased about 12.54% in RCP4.5 scenario and 27.84% in RCP8.5 scenario in Fut2. Considering that RV50 of ASOS is related with flood, more than 50% of stations are projected to be exposed to more intense floods under RCP scenarios.

5. Summary and discussion

This study has assessed the future change of extreme precipitation over S. Korea. The high-resolution (12.5 km) regional projection data under RCP4.5 and RCP8.5 scenario is produced by 5 institutes with 5 different RCMs using the Global RCP projection of HadGEM2-AO participating in CMIP5 as the lateral boundary condition produced by NIMR. The GEV statistical method is used to estimate the intensity of extreme precipitation. Firstly, we assess the performance of HadGEM2-AO and the 5 RCMs with RMSE and bias in comparison to observation using the historical experiment. The results show that the summer precipitation dry bias of HadGEM2-AO is decreased after dynamical downscaling, indicating that estimation of extreme precipitation is more reasonable with this GCM-RCMs model chain than with GCM alone. Also, it is shown that every RCM has different biases both spatially and temporally, despite using the same lateral boundary condition. Under RCP4.5/8.5 scenarios, precipitation intensity and 95th precipitation are projected to increase.

The change in daily precipitation with respect to various intensity ranges clearly shows a decreasing sign for low-intensity precipitation but an increasing sign for high-intensity precipitation in all RCM projections. With this result, we estimate the future changes of extreme precipitation. As GHG forcing is enhanced and the return period increased, the maximum GEV value over S. Korea is increased. The median values in Fut2 are larger than those in Fut1. Meanwhile, the difference of median among the 5 RCMs is more than 100 mm d^{-1} and the intensity and spatial pattern of RV50 vary widely among the 5 models. Moreover, the RCMs show relatively smaller quantity of daily extreme precipitation than does ASOS. Thus, it is better to investigate the future change of extreme precipitation as a ratio with respect to historical rather than as a deterministic value. RV50 is shown to be increased, although some areas show decreasing extreme precipitation under climate change. The Fut2 period under RCP8.5 scenario shows the most notable increase of RV50. However, the RV50 intensity shows the bias of each model and the spatial distributions of RV50 changes also vary from model to model (not shown). Moreover, these results are dependent on the period of analysis and number of ensemble members. Therefore, the effect of climate change on S. Korea cannot be specified deterministically because of these spatiotemporal uncertainties with only 5 ensemble members. Therefore, we propose the RV50 change (%) in terms of confidence interval. According to the projections by the 5 RCMs, we expect that S. Korea will experience an increase of extreme precipitation from −19.45% to 134.8% under RCP8.5 at the 90% confidence level. For the median, RCP4.5 Fut1 seems to have a similar level of intensity whereas RCP8.5 Fut2 presents a RV50 increase of 27.84% compared to historical experiment.

In addition to the result on extreme precipitation projection, we also noticed the risk in using only one GCM and one RCM model chain to assess the changes of extreme precipitation. It is shown that different RCMs could make diverse spatial patterns of RV50 change although we use 1 driving GCM, which is in accordance with the result of Fowler et al. (2007), who suggested that RCMs moderate and influence spatial patterns in multi-model ensemble study for estimating the change of extreme precipitation. In spite of the advantage afforded by using various RCMs, the use of only one driving GCM still retains the limitation. Moreover, the uncertainty of future projection could arise due to the model and schemes used, the analysis period and the target domains (Leduc and Laprise, 2008; Separovic et al., 2012). Thus, an ensemble approach based on the multi-GCM and multi-RCM will be necessary in future research to assess the impact of regional climate change over S. Korea with high confidence.

Acknowledgements. This work was funded by the Korea Meteorological Administration Research and Development Program under grant KMIPA 2015-2081 and the Rural Development Administration Cooperative Research Program for Agriculture Science and Technology Development Project PJ009953.

Edited by: John McGregor

References

Ahn, J. B., J. Lee, and E. S. Im, 2012: The reproducibility of surface air temperature over South Korea using dynamical downscaling and statistical correction. *J. Meteor. Soc. Japan*, **90**, 493-507.

______, Y. W. Choi, S. R. Jo, and J. Y. Hong, 2014: Projection of 21st Century Climate over Korean Peninsula: Temperature and Precipitation Simulated by WRFV3.4 Based on RCP4.5 and 8.5 scenarios. *Atmosphere*, **24**, 541-554 (in Korean with English abstract).

Baek, H. J., and Coauthors, 2013: Climate change in the 21st century simulated by HadGEM2-AO under Representative Concentration Pathways. *Asia-Pac. J. Atmos. Sci.*, **49**, 603-618.

Chen, J., F. P. Brissette, and R. Leconte, 2011: Uncertainty of downscaling method in quantifying the impact of climate change on hydrology. *J. Hydrol.*, **401**, 190-202.

Collins, M., and Coauthors, 2013: Long-term Climate Change: Projections, Commitments and Irreversibility. *Climate Change 2013: The Physical Science Basis. Contribution of Working Group I to the Fifth Assessment Report of the Intergovernmental Panel on Climate Change,* T. F. Stocker et al. Eds., Cambridge University Press, 1029-1136.

Dosio, A., H. J. Panitz, M. Schubert-Frisius, and D. Lüthi, 2015: Dynamical downscaling of CMIP5 global circulation models over CORDEX-Africa with COSMO-CLM: evaluation over the present climate and analysis of the added value. *Clim. Dynam*., **44**, 2637-2661.

Ehret, U., E. Zehe, V. Wulfmeyer, K. Warrach-Sagi, and J. Liebert, 2012: HESS Opinions "Should we apply bias correction to global and regional climate model data?" *Hydrol. Earth Syst. Sci*., **16**, 3391-3404.

Emmanouil, F., D. Philippe, and S. Bastin, 2013: Dynamical downscaling of IPSL-CM5 CMIP5 historical simulations over the Mediterranean: benefits on the representation of regional surface winds and cyclogenesis. *Clim. Dynam*., **40**, 2497-2513.

Fisher, R. A. and L. H. C. Tippett, 1928: Limiting forms of the frequency distribution of the largest or smallest member of a sample. *Proc. Camb. Philos. Soc,*. **24**, 180-190.

Fowler, H. J., M. Ekström, S. Blenkinsop, and A. P. Smith, 2007: Estimating change in extreme European precipitation using a multimodel ensemble. *J. Geophys. Res*., **112**, D18104, doi:10.1029/2007-JD008619.

Frei, C., J. H. Christensen, M. Déqué, D. Jacob, R. G. Jones, and P. L. Vidale, 2003: Daily precipitation statistics in regional climate models: Evaluation and intercomparison for the European Alps. *J. Geophys. Res.*, **108**, 4124, doi:10.1029/2002JD002287.

Gutowski, W. J., K. A. Kozak, R. W. Arritt, J. H. Christensen, J. C. Patton, and E. S. Takle, 2007: A possible constraint on regional precipitation intensity changes under global warming. *J. Hydrometeor.*, **8**, 1382-1396.

Hanel, M., and T. A. Buishand, 2011: Analysis of precipitation extremes in an ensemble of transient regional climate model simulations for the Rhine basin. *Clim. Dynam.*, **36**, 1135-1153.

Harding, K. J., P. K. Snyder, and S. Liess, 2013: Use of dynamical downscaling to improve the simulation of Central U.S. warm season precipitation in CMIP5 models*, J. Geophys. Res.*, **118**, 522-536.

Heinrich, G., and A. Gobiet, 2011: The future of dry and wet spells in Europe: A comprehensive study based on the ENSEMBLES regional climate models. *Int. J. Climatol.*, **32**, 1951-1970.

Hong, J. Y., and J. B. Ahn, 2015: Changes of Early Summer Precipitation in the Korean Peninsula and Nearby Regions Based on RCP Simulations. *J. Climate*, **28**, 3557-3578.

Hong, S. Y., S. G. Oh, M. S. Suh, D. K. Lee, J. B. Ahn, and H. S. Kang, 2013: Future Climate Changes over North-East Asian Region Simulated by RegCM4 Based on the RCP Scenarios. *Clim. Res.*, **8**, 27-44 (in Korean with English abstract).

Hosking, J. R. M., and J. R. Wallis, 1997: *Regional frequency analysis: an approach based on L-moments.* Cambridge University Press, 224 pp.

Im, E. S., E. H. Park, W. T. Kwon, and F. Giorgi, 2006: Present climate simulation over Korea with a regional climate model using a one-way nested system. *Theor. Appl. Climatol.*, **86**, 187-200.

______, W. T. Kwon, J. B. Ahn, and F. Giorgi, 2007: Multi-decadal scenario simulation over Korea using a one-way doublenested regional climate model system. I. Recent climate simulation (1971-2000). *Clim. Dynam.*, **28**, 759-780.

______, W. J. Gutowski, and F. Giorgi, 2008: Consistent changes in twenty-first century daily precipitation from regional climate simulations for Korea using two convection parameterizations. *Geophys. Res. Lett.*, **35**, L14706.

______, I. W. Jung, and D. H. Bae, 2011: The temporal and spatial structure of recent and future trends in extreme indices over Korea from a regional climate projection. *Int. J. Climatol.*, **31**, 72-86.

______, B. J. Lee, J. H. Kwon, S. R. In, and H. O. Han, 2012: Potential increase of flood hazards in Korea due to global warming from a high-resolution regional climate simulation. *Asia-Pac. J. Atmos. Sci.*, **48**, 107-113.

______, J. B. Ahn, and S. R. Jo, 2015: Regional climate projection over South Korea simulated by the HadGEM2-AO and WRF model chain under RCP emission scenarios. *Clim. Res.*, **63**, 249-266.

Jankov, I., W. Gallus, M. Segal, B. Shaw, and S. Koch, 2005: The impact of different WRF model physical parameterizations and their interactions on warm season MCS rainfall. *Wea. Forecast*, **20**, 1048-1060.

Jeong, H. I., D. Y. Lee, K. Ashok, J. B. Ahn, J. Y. Lee, J. J. Luo, J. K. Schemm, H. H. Hendon, K. Braganza, and Y. G. Ham, 2012: Assessment of the APCC coupled MME suite in predicting the distinctive climate impacts of two flavors of ENSO during boreal winter. *Clim. Dynam*., **39**, 475-493.

Kirtman, B., and Coauthors, 2013: Near-term Climate Change: Projections and Predictability. *Climate Change 2013: The Physical Science Basis. Contribution of Working Group I to the Fifth Assessment Report of the Intergovernmental Panel on Climate Change,* T. F. Stocker et al. Eds., Cambridge University Press, 953-1028.

Kryjov, V. N., 2012: Seasonal climate prediction for North Eurasia. *Environ. Res. Lett.,* **7**, 015203, doi:10.1088/1748-9326/7/1/015203.

Kug, J. S., L. Y. Lee, and I. S. Kang, 2008: Systematic error correction of dynamical seasonal prediction of sea surface temperature using a stepwise pattern project method. *Mon. Wea. Rev*., **136**, 3501-3512.

Leduc, M., and R. Laprise, 2008: Regional climate model sensitivity to domain size. *Clim. Dynam.,* **32**, 833-854.

Lee, D. K., H. R. Kim, and S. Y. Hong, 1998: Heavy rainfall over Korea during 1980-1990. *Korean J. Atmos. Sci.*, **1**, 32-50.

Lee, D. Y., J. B. Ahn, K. Ashok, and A. Alessandri, 2013a: Improvement of grand multi-model ensemble prediction skills for the coupled models of APCC/ENSEMBLES using a climate filter. *Atmos. Sci. Lett*., **14**, 139-145.

______, ______, and ______, 2013b: Improvement of multi-model ensemble seasonal prediction skills over East Asian summer monsoon region using a climate filter concept*. J. Appl. Meteorol.*, **52**, 1127-1138.

Lee, J. W., and S. Y. Hong, 2014: Potential for added value to downscaled climate extremes over Korea by increased resolution of a regional climate model. *Theor. Appl. Climtol*., **117**, 667-677.

______, ______, E. C. Chang, M. S. Suh, and H. S. Kang, 2014: Assessment of future climate change over East Asia due to the RCP scenarios downscaled by GRIMs-RMP. *Clim. Dynam.*, **42**, 733-747.

Martin, G. M., and R. C. Levine, 2012: The influence of dynamic vegetation on the present-day simulation and future projections of the South Asian summer monsoon in the HadGEM2 family. *Earth Syst. Dynam.*, **3**, 245-261.

Mehran, A., A. AghaKouchak, and T. J. Phillips, 2014: Evaluation of CMIP5 continental precipitation simulations relative to satellite-based gauge-adjusted observations. *J. Geophys. Res.*, **119**, 1695-1707.

Meinshausen, M., and Coauthors, 2011: The RCP Greenhouse Gas Concentrations and their Extension from 1765 to 2300. *Climatic Change*, **109**, 213-241.

Moss, R. H., and Coauthors, 2010: The next generation of scenarios for climate change research and assessment. *Nature*, **463**, 747-756.

O'Gorman, P. A., and T. Schneider, 2009: The physical basis for increases in precipitation extremes in simulations of 21st-century climate change. *Proc. Natl. Acad. Sci. U.S.A.*, **106**, 14773-14777.

Oh, S. K., J. H. Park, S. H. Lee, and M. S. Suh, 2014: Assessment of the RegCM4 over East Asia and future precipitation change adapted to the RCP scenarios. *J. Geophys. Res.*, **119**, 2913-2927.

Peng, P., A. Kumar, H. van den Dool, and A. G. Barnston, 2002: An analysis of multimodel ensemble predictions for seasonal climate anomalies. *J. Geophys. Res.*, **107**, 4710, doi:10.1029/2002JD002712.

Seo, Y. A., Y. Lee, J. S. Park, M. K. Kim, C. Cho, and H. J. Baek, 2015: Assessing changes in observed and future projected precipitation extremes in South Korea. *Int. J. Climatol.*, **35**, 1069-1078.

Separovic, L., R. Elía, and R. Laprise, 2012: Impact of spectral nudging and domain size in studies of RCM response to parameter modification. *Clim. Dynam.*, **38**, 1325-1343.

Shindell, D. T., A. Voulgarakis, G. Faluvegi, and G. Milly, 2012: Precipitation response to regional radiative forcing. *Atmos. Chem. Phys.*, **12**, 6969-6982.

Sillmann, J., V. V. Kharin, F. W. Zwiers, X. Zhang, and D. Bronaugh, 2013: Climate extremes indices in the CMIP5 multimodel ensemble: Part 2. Future climate projections. *J. Geophys. Res.*, **118**, 2473-2493.

Sun, Y., S. Solomon, A. Dai, and R. W. Portmann, 2007: How often will it rain? *J. Climate*, **20**, 4801-4818.

Taylor, K. E., R. J. Stouffer, and G. A. Meehl, 2012: An overview of CMIP5 and the experiment design. *Bull. Amer. Meteorol. Soc.*, **93**, 485-498.

Teutschbein, C., and J. Seibert, 2012a: Bias correction of regional climate model simulations for hydrological climate-change impact studies: Review and evaluation of different methods. *J. Hydrol.*, **456**, 12-29.

______, and ______, 2012b: Is bias correction of Regional Climate Model (RCM) simulations possible for non-stationary conditions? *Hydrol. Earth Syst. Sci. Discuss.*, **9**, 12765-12795.

Wilks, D. S., 2011: *Statistical Methods in the Atmospheric Sciences*. Academic Press, 704 pp.

Xu, Y., C. H. Xu, X. J. Gao, and Y. Luo, 2009: Projected changes in temperature and precipitation extremes over the Yangtze River Basin of China in the 21st century. *Quat. Int.*, **208**, 44-52.

Yu, E., J. Sun, H. Chen, and W. Xiang, 2015: Evaluation of a high-resolution historical simulation over China: climatology and extremes. *Clim. Dynam.*, **45**, 2013-2031.

Zwiers, F. W., X. Zhang, and Y. Feng, 2011: Anthropogenic influence on long return period daily temperature extremes at regional scales. *J. Climate*, **24**, 881-892.